Textures and Microstructures, Vol. 32, pp. 355–367
Reprints available directly from the publisher
Photocopying permitted by license only

© 1999 OPA (Overseas Publishers Association) N.V.
Published by license under
the Gordon and Breach Science
Publishers imprint.
Printed in Malaysia.

VARIATION OF PLASTIC STRAIN RATIOS OF α-BRASS SHEET WITH TENSILE STRAIN

HYO-TAE JEONG, SEUNG-HYUN HONG
and DONG NYUNG LEE*

Division of Materials Science and Engineering, Seoul National University, Seoul 151-742, Korea

(Received in final form 28 September 1997)

A study has been made of the changes in the instantaneous plastic strain ratios along various directions of α-brass sheet as a function of tensile strain. The α-brass sheet was fabricated by 88% cold rolling and subsequent annealing at 450°C for 1.5 h, which lead to complete recrystallization. The recrystallization texture of the α-brass sheet could be approximated by {110}⟨110⟩. The plastic strain ratio along the rolling direction decreased with increasing tensile strain, whereas those along 45°, 90° to the rolling direction were almost independent of tensile strain. The results were in agreement with those calculated using the recrystallization textures based on the Taylor–Bishop–Hill full constraints model.

Keywords: α-brass; Instantaneous plastic strain ratio; Texture; Tensile strain; Taylor–Bishop–Hill theory; Full constraints model

1. INTRODUCTION

Variation of the plastic strain ratio or the Lankford parameter with tensile strain has been reported by many investigators (Hu, 1975a,b; Truzkowski, 1976; Arthey and Hutchinson, 1981; Liu, 1983). In order to understand the phenomenon, it is convenient to classify the plastic strain ratio into the conventional and instantaneous plastic strain ratios.

* Corresponding author.

The conventional plastic strain ratio, R_e, suggested by Lankford is defined by

$$R_e = \varepsilon_w/\varepsilon_t = -\varepsilon_w/(\varepsilon_l + \varepsilon_w) \tag{1}$$

where ε_w, ε_t and ε_l are the true plastic strains in the width, thickness and tensile directions, respectively. It is noted that no volume change in plastic deformation is assumed in Eq. (1). The R_e value is usually calculated from the measured ε_w and ε_l values, and is widely used to evaluate deep drawability of sheet metals.

If the R_e value is independent of tensile strain, the ε_l–ε_w curve will show a linear relation as shown in Fig. 1, where the slope of line is given by $-R_e/(R_e+1)$. If there is no error, the line must start from zero point. However, the measured ε_l–ε_w results often show relations as in Fig. 2. The first case shows a linear relation of ε_l–ε_w except in the initial stage, whereas the second case shows no linear relation at all. The first case may again be classified into two cases as shown in Fig. 3(a) and (b). For Fig. 3(a) and (b), R_e will behave as shown in Fig. 3(c) and (d) as a function of tensile strain ε_l.

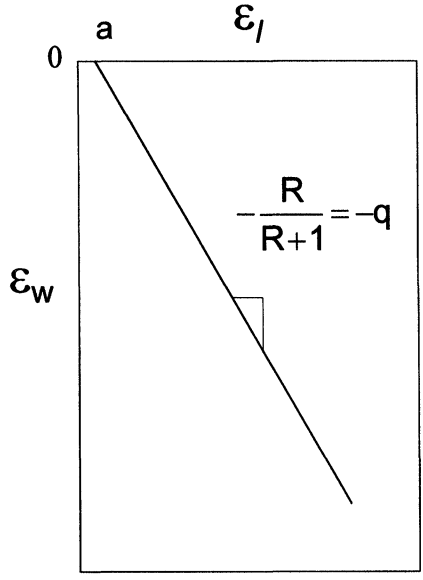

FIGURE 1 Schematic drawing of width strain ε_w as function of tensile strain ε_l when plastic strain ratio R is independent of strain.

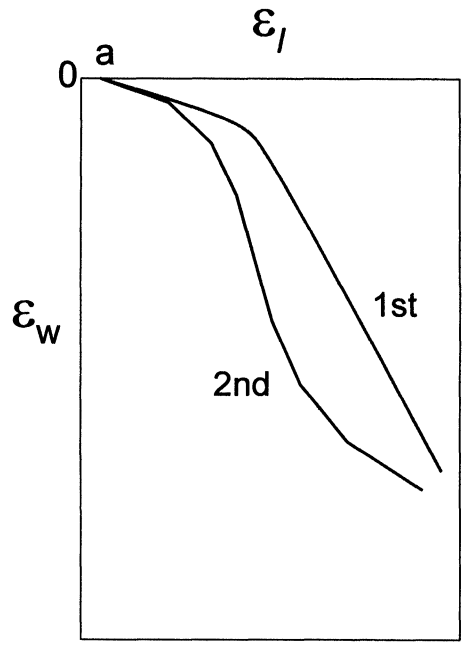

FIGURE 2 Schematic drawing of width strain ε_w as function of tensile strain ε_l when plastic strain ratio R varies with strain.

If the plastic strain ratio is defined by the instantaneous slope of the ε_l–ε_w curve, the results in Fig. 3(a) and (b) will give rise to the curves R_i in Fig. 3(c) and (d). For the second curve in Fig. 2, R_e and R_i are defined in Fig. 4 (Welch *et al.*, 1983; Lake *et al.*, 1988). R_i is called the instantaneous plastic strain ratio and is expressed as

$$R_i = d\varepsilon_w/d\varepsilon_t. \tag{2}$$

The instantaneous plastic strain ratio corresponds to the quantity that is usually calculated from the texture.

The objective of this article is to measure the instantaneous plastic strain ratio of α-brass sheet as a function of tensile strain and to discuss the results based on its textures.

2. EXPERIMENTAL METHOD

The 0.8 mm thick α-brass sheet (Cu-28% Zn) was made by 88% cold rolling at room temperature, followed by annealing at 450°C for 1.5 h.

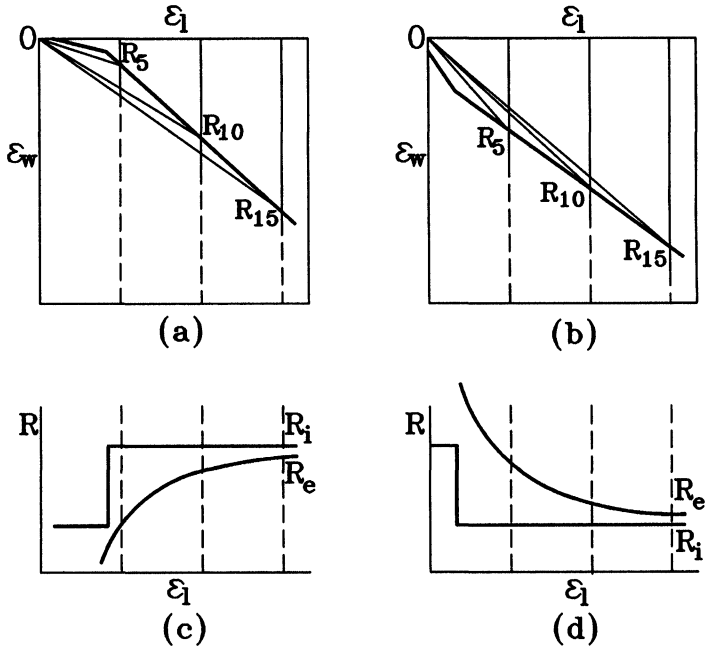

FIGURE 3 Difference between conventional plastic strain ratio R_e and instantaneous plastic strain ratio R_i.

The tensile specimens of ASTM E8 subsize were prepared by milling the α-brass sheets.

The width and longitudinal displacements during tensile testing were instantaneously measured using two extensometers. The longitudinal displacement was measured up to 10 mm at intervals of 4.8 μm, while the width displacement was measured up to 1.5 mm at intervals of 0.69 μm, which is equivalent to about 1000 data at a tensile strain of 0.2. The measured displacements were used to calculate strains, from which the plastic strains were obtained by subtracting the elastic strains. The elastic strains were calculated using the following equation:

$$\varepsilon_w^e = -\nu\varepsilon_l^e = \frac{\nu}{E}\sigma(\varepsilon_l) \tag{3}$$

where superscript e represents elastic property, and ν is Poisson's ratio. Equation (3) holds for isotropic elastic materials. Therefore, the

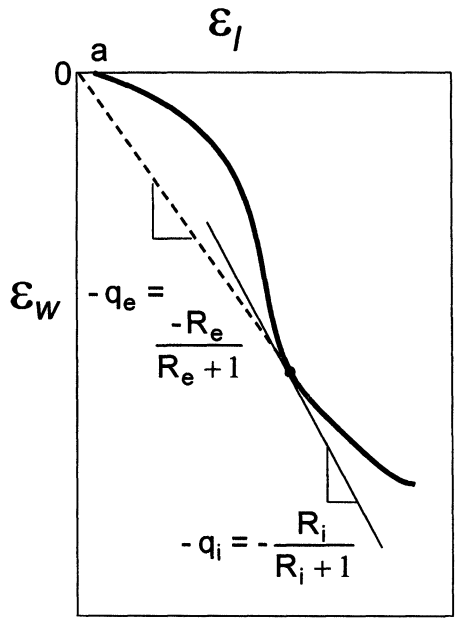

FIGURE 4 Definition of conventional plastic strain ratio R_e and instantaneous plastic strain ratio R_i, where $-q_e$ and $-q_i$ are slopes of dashed and sold lines.

effect of elastic anisotropy on the plastic strains was neglected. Young's modulus and Poisson's ratio used are 115 GPa and 0.343, respectively.

In order to reduce the noise of the measured data, an instantaneous plastic strain ratio was calculated from the slope of a quadratic equation best fitting 50 data obtained from a tensile strain range of $\pm 0.5\%$.

The textures of the annealed specimens were measured up to the reflection angle of 80° using a Schultz pole figure device. Incomplete pole figures of (111), (200) and (220) for the α-brass specimen were used to calculate ODFs using the series expansion method with $L_{\max} = 22$ (Bunge, 1982).

3. RESULTS AND DISCUSSION

Figure 5 shows the measured width strains and the R_i values along 0°, 45° and 90° to the rolling direction of α-brass specimens as a function of

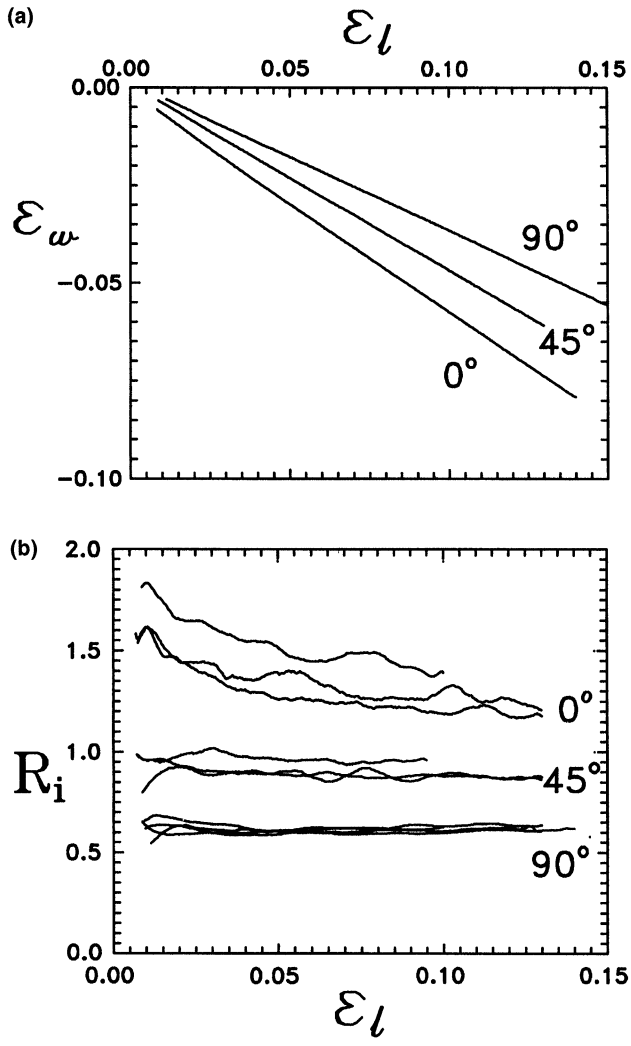

FIGURE 5 Measured (a) width strain ε_w and (b) instantaneous plastic strain ratio R_i of annealed α-brass sheet as function of tensile strain ε_l.

tensile strain. The R_i values of 45° and 90° specimens are independent of the tensile strain, whereas the R_i values of 0° specimen decreases with increasing tensile strain.

Figure 6 shows the measured (111) and (200) pole figures of the annealed specimen. Figure 7 shows the measured (111) and (200) pole

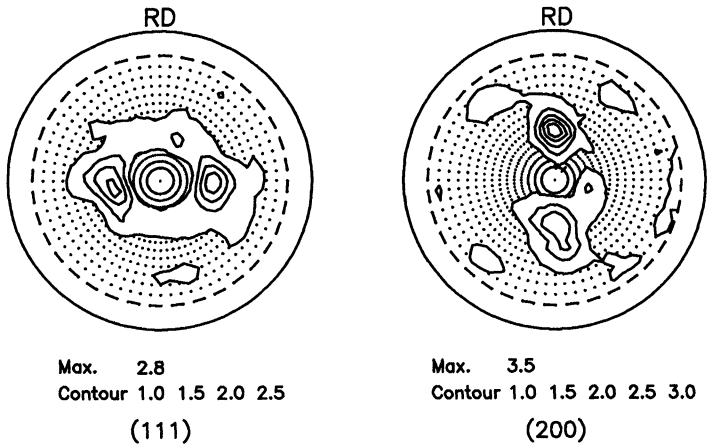

FIGURE 6 Measured (111) and (200) pole figures of annealed α-brass sheet.

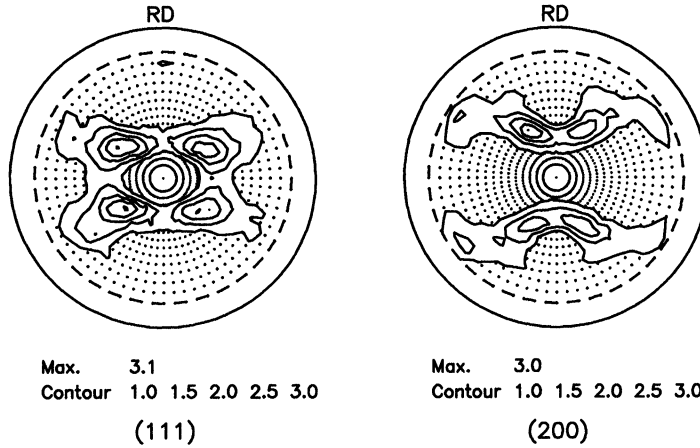

FIGURE 7 Measured (111) and (200) pole figures of α-brass sheet tensile deformed by 33%.

figures of the specimen tensile deformed by 33% along the rolling direction. The ODFs calculated using the pole figures in Figs. 6 and 7 are shown in Fig. 8(a) and (b), respectively. The texture of the annealed specimen may be approximated by the $\{110\}\langle 110\rangle$ orientation and the texture of the tensile deformed specimen may be approximated by the $\{110\}\langle 111\rangle$ orientation.

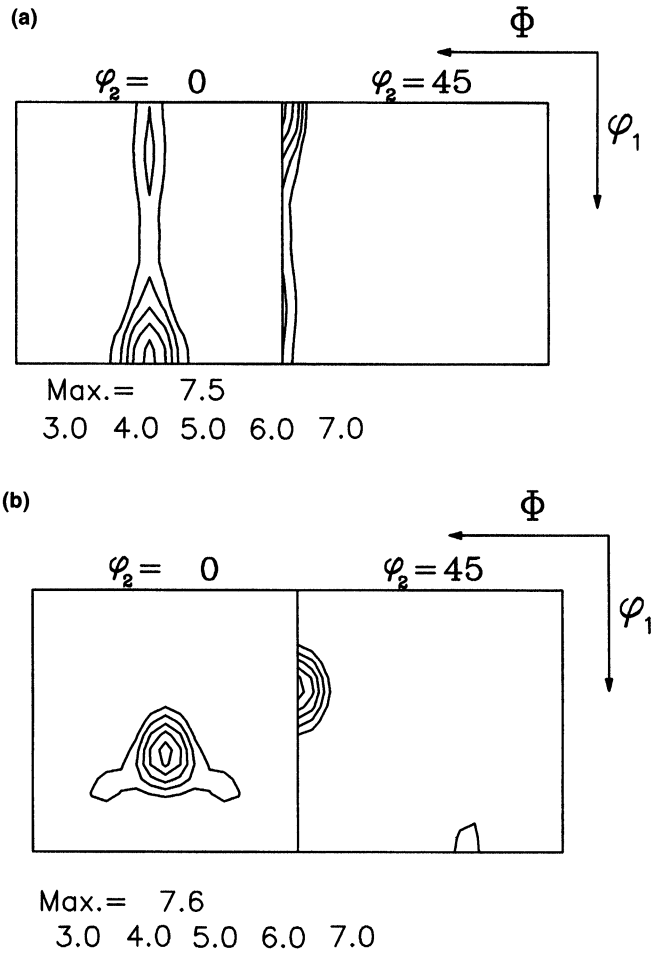

FIGURE 8 ODFs at $\varphi_2 = 0$ and 45° sections of α-brass sheet (a) annealed at 450°C for 1.5 h after 88% rolling and (b) tensile deformed by 33%.

The R_i values of the annealed and tensile deformed specimens were calculated as a function of angle to the rolling direction using Bunge's method (Bunge, 1982) based on the measured textures (Fig. 9). The calculated R_i values of the annealed specimen along 0°, 45° and 90° to the rolling direction are 1.60, 0.86 and 0.46, respectively, which are in good agreement with the measured R_i values at the small tensile strain (Fig. 5(b)). The calculated R_i values of the tensile deformed specimens

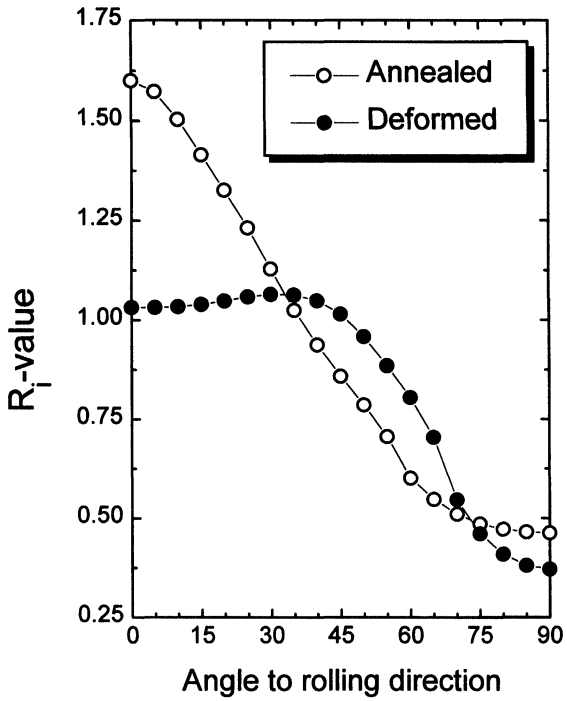

FIGURE 9 Instantaneous plastic strain ratio calculated using Bunge's method as function of angle to rolling direction for annealed and tensile deformed α-brass sheet.

along 45° and 90° to the rolling direction are similar to those of the annealed specimens, whereas the R_i value along the rolling direction decreases drastically. This decrease of R_i value along the rolling direction was attributed to the observed texture change from $\{110\}\langle 110\rangle$ to $\{110\}\langle 111\rangle$.

For qualitative understanding of the R_i results, the development of texture was calculated as a function of tensile strain, from which the R_i was calculated. The annealing texture of α-brass sheet was expressed as the Gaussian function of $\{110\}\langle 110\rangle$ orientation with a half width of 30° and the calculated pole figures and ODF are shown in Figs. 10 and 11(a), respectively. Therefore, the annealing texture of 45° and 90° specimens was expressed as Gaussian functions of $\{110\}\langle 11\sqrt{2}\rangle$ and $\{110\}\langle 001\rangle$ orientations with a half width of 30°.

The tensile deformation textures were calculated using the Taylor–Bishop–Hill full constraints model, in which the slip systems were

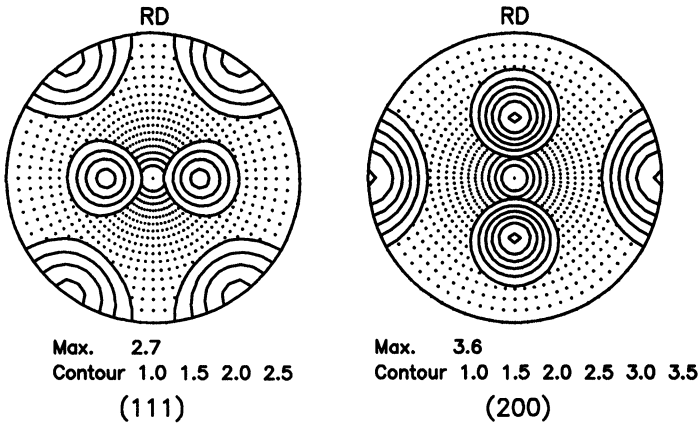

FIGURE 10 (111) and (200) pole figures of $\{110\}\langle 110\rangle$ texture expressed as Gaussian function with $L_{max=22}$ and $\omega_o = 30°$.

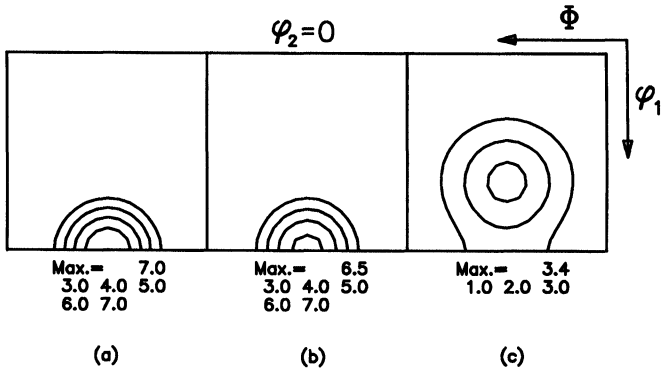

FIGURE 11 ODFs at $\varphi_2 = 0°$ section of α-brass sheet tensile deformed along the rolling direction, which were calculated using Taylor–Bishop–Hill full constraint model. (a) $\varepsilon_1 = 0.0$, (b) $\varepsilon_1 = 0.4$, (c) $\varepsilon_1 = 1.5$.

selected using the random choice of linear programming method (Van Houtte, 1981). The calculated deformation textures are shown in Figs. 11–13. The $\{110\}\langle 110\rangle$ and $\{110\}\langle 11\sqrt{2}\rangle$ orientation of 0° and 45° specimens are rotated to $\{110\}\langle 111\rangle$ orientation during tensile deformation, while the $\{110\}\langle 001\rangle$ orientation of 90° specimen is stable. The calculated annealing and deformation textures were used to calculate the R_i values using Bunge's method. The calculated results are shown in Fig. 14. It can be seen that the 0° specimen of $\{110\}\langle 110\rangle$ orientation yields R_i values which strongly decrease with increasing tensile strains, whereas

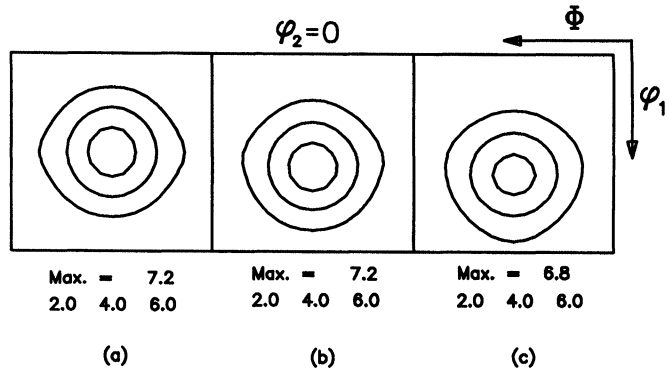

FIGURE 12 ODFs at $\varphi_2 = 0°$ section of α-brass sheet tensile deformed along 45° to rolling direction, which were calculated using Taylor–Bishop–Hill full constraint model. (a) $\varepsilon_l = 0.0$, (b) $\varepsilon_l = 0.4$, (c) $\varepsilon_l = 1.5$.

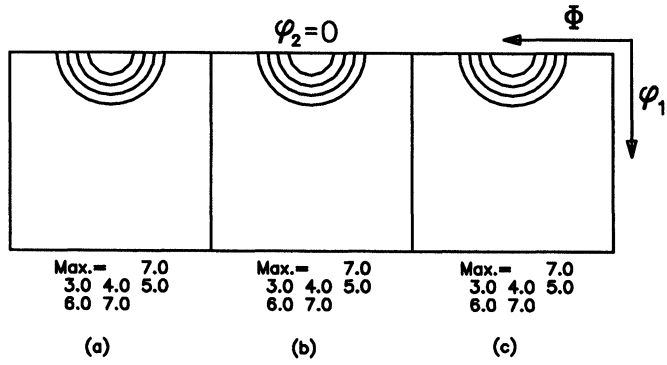

FIGURE 13 ODFs at $\varphi_2 = 0°$ section of α-brass sheet tensile deformed along 90° to rolling direction, which were calculated using Taylor–Bishop–Hill full constraint model. (a) $\varepsilon_l = 0.0$, (b) $\varepsilon_l = 0.4$, (c) $\varepsilon_l = 1.5$.

the R values of the 45° and 90° specimens are virtually independent of the tensile strain.

These results are in qualitative agreement with the measured R_i values. Therefore, the variations of R_i with tensile strain can be attributed to the texture change in α-brass sheets during tensile deformation.

4. CONCLUSION

The instantaneous plastic strain ratios and textures of α-brass sheets were measured as functions of tensile strain and angle to the rolling

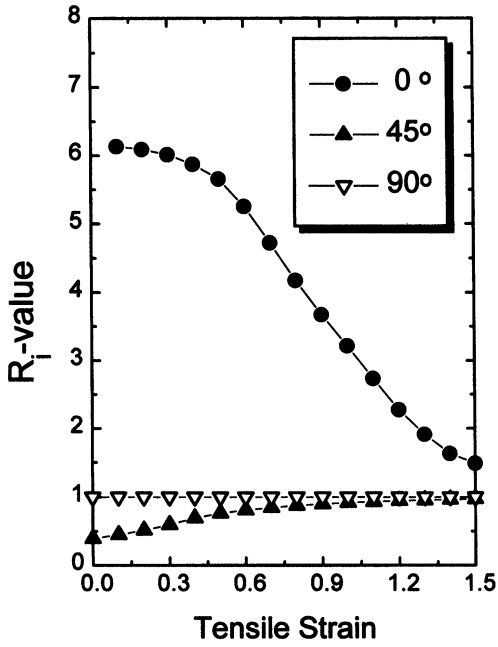

FIGURE 14 Variation of instantaneous plastic strain ratio calculated based on development of deformation texture using Bunge's method as function of tensile strain for α-brass sheet.

direction. The recrystallization texture of α-brass sheet rolled by 88% and annealed at 450°C for 1.5 h was approximated by $\{110\}\langle 110\rangle$, which changed to the texture approximated by $\{110\}\langle 111\rangle$ after a tensile strain of 33%. The R_i values of specimens along 45° and 90° to the rolling direction were almost independent of tensile strain, whereas that of the 0° specimen decreased with increasing tensile strain. The R_i results are attributed to the texture variation during tensile deformation.

Acknowledgments

This study has been supported by Korea Science and Engineering Foundation through RETCAM, Seoul National University.

References

Arthey, R.P. and Hutchinson, W.B. (1981) *Metall. Trans. A*, **12**, 1817.
Bunge, H.J. (1982) "Texture Analysis in Materials Science" Butterworths, London, p. 330

Hu, H. (1975a). *Metall. Trans. A*, **6**, 2307.
Hu, H. (1975b). *Metall. Trans. A*, **6**, 945.
Lake, J.S.H., Willis, D.J. and Fleming, H.G. (1988). *Metall. Trans. A*, **19**, 2805.
Liu, Y.C. (1983). *Metall. Trans. A*, **14**, 1199.
Truzkowski, W. (1976). *Metall. Trans. A*, **7**, 327.
Van Houtte, P. (198l). ICOTOM 6, *Tokyo*, **1**, 428.
Welch, P.I., Ratke, L. and Bunge, H.-J. (1983). *Z. Metallkde.*, **74**(4), 233.